COMPARISON OF DIFFERENTS TURBULENCE MODELS FOR INDOOR AIRFLOW COMPUTATIONS

Guilherme Anrain Lindner, guilherme@cardinal.com.br
Roberto Mathias Susin, contato@laboratorioderobotica.com
Viviana Cocco Mariani, viviana.mariani@pucpr.br
Kátia Cordeiro Mendonça, k.mendonca@pucpr.br

Mechanical Engineering Department
Pontifical Catholic University of Parana – PUCPR
80215-901 – Curitiba, PR, Brazil

Abstract. *The goal of this work is to investigate the ability of three eddy viscosity turbulent model, i.e the standard k-ε, the RNG k-ε and the k-ω, in predicting the three-dimension airflow in a room under forced convection. The experimental data from Nielsen (1990), which represents a large room where the air enters horizontally at the top of one side and leaves the room at the bottom of the opposite side, was used to validate the models. The results for Reynolds number 5,000 are presented for mean velocity profiles in two planes of the room with two inlet arrangements. It has been found that velocity profiles calculated using k-ε and k-ω turbulence models agree better with experimental data than those using the RNG k-ε model. It should be mentioned that a full assessment of the turbulence models in the airflow in room would require a comparison using other numerical grids.*

Keywords*: Horizontal jet, k-ε model, RNG k-ε model, k-ω model, turbulence.*

1. INTRODUCTION

Air-conditioning systems are supposed to provide comfort and health indoor air conditions in confined spaces. However, these devices can produce gradients of the air properties that may cause a sensation of discomfort even if the occupants' global thermal perceptions of the indoor environment remain satisfactory. Consequently, a detailed description of the air distribution is necessary to accurately evaluate thermal comfort in conditioned rooms.

Computational Fluid Dynamics (CFD) can give detailed information about the airflow pattern and the air properties distribution. Although recent computational progresses have allowed this method to become very popular, the choice of the more appropriate turbulence model still remains difficult to the user. In the context of this work, predicting the airflow in a room, a number of important studies can be cited as follow.

Nielsen *et al*. (1978) employed the standard *k-*ε model to simulate in two-dimensions a rectangular room ventilated by a horizontal jet. The numerical mean velocity profiles agreed well, in the order of ± 5%, with the experimental results obtained by the authors and those available in the literature of that time. The authors emphasized the importance of the jet inlet conditions for correctly simulating the air movement in the room.

Chen (1995) examined the performance of five *k-*ε models in predicting typical turbulent indoor airflow, comparing the numerical results from two-dimension simulations to experimental data. He concluded that the five *k-*ε models could predict the mean velocity satisfactory but not the instantaneous velocity because of their underlying assumption of isotropic turbulence, and recommended the RNG *k-*ε model from Yakhot *et al*. (1992) for typical indoor airflow. The author also evaluated the performance of three Reynolds-Stress models to predict airflow patterns in rooms (Chen, 1996). All three Reynolds-Stress models agreed better with the experimental results than the standard *k-*ε model. Additionally, they could predict the existence of a secondary recirculation that is not possible with an isotropic model like the standard *k-*ε. On the other hand, besides their complexity, Chen (1996) showed the Reynolds-Stress models are much more time consuming than the standard *k-*ε model.

Chen and Xu (1998) proposed a zero equation turbulence model for indoor airflow simulation. They compared the performance of this simple model to that of standard *k-*ε model in describing natural, forced and mixed convection and the particular case of displacement ventilation. Although the proposed zero equation model was less accurate than the standard *k-*ε model, it provided reasonable results while consuming much less computational time than the standard *k-*ε model.

Voigt (2000) used the experimental results from Nielsen (1978) to validate an in-house CFD code and to compare five eddy viscosity turbulence models: two *k-*ε models from Launder and Spalding (1974) and Launder and Sharma (1974) and three *k-*ω models from Wilcox (1988) and Menter (1993, 1994). The comparative analysis showed that the *k-*ε models agreed better with the experimental results, and that the shear stress transport *k-*ω model (Menter, 1994) poorly predicted the studied airflow.

Xu and Chen (2001a) presented a two-layer model to predict turbulent indoor airflow under natural, forced and mixed convection. The proposed model is composed of a near-wall one equation model for the near-wall region, which combines one equation model more appropriated for forced convection and another one more appropriated for natural convection, and the standard k-ε model for the outer-wall region. The ability of this model in predicting natural, forced and mixed convection was evaluated by Xu and Chen (2001b). On the whole, the analysis showed that the mean properties agreed much better with experimental and DNS (Direct Numerical Simulation) data than the fluctuating ones for all studied cases. The advantage of the proposed model over the standard k-ε and Low-Reynolds k-ε models mainly lies in the need of less computational time.

Moureh and Flick (2003) used the standard k-ε model, the RNG k-ε model and Reynolds-Stress Equation Model (RSM) to study the airflow pattern in a long room where the inlet and the outlet of air were placed in the same wall. The two regions of circulation that appears in this particular case could only be predicted by the RSM model.

Schälin and Nielsen (2004) numerically investigated the three-dimensional effects of wall jets in a short and a long room using two high Reynolds turbulence models: the standard k-ε model and the standard RSM (Launder, 1989). The authors showed that the wall jet behavior, like the growth rate parallel to the wall, can be better represented by the RSM model.

It has been shown in the above literature review that typical indoor air motion can be quite well predict by RSM, while the eddy viscosity models predict satisfactory the mean flow and poorly its fluctuations and secondary flows. Nevertheless, as RSM are complex, numerically instable and time consuming, the eddy viscosity models seem to be more appropriate for building ventilation system design and for this reason this work is focused on them.

With the exception of Schälin and Nielsen's work, none of the previously cited papers dealt with the three-dimensional effects of the flow. Therefore, the goal of this work is to investigate the ability of three isotropic models (standard k-ε, *RNG* k-ε *and* k-ω) in predicting the three-dimension flow in a room under forced convection. In order to perform this analysis the numerical mean velocity profiles for two planes of the room with two inlet arrangements are compared to the experimental data from Nielsen (1990).

2. MODEL DESCRIPTION

2.1 Governing equations

Reynolds (1894) decomposed the Navier-Stokes equations in two parties, one related to the average value of the velocity vector and another related to its fluctuation, and applied the time average operator on them to study turbulent flows. The resulting set of equations is known as Reynolds Average Navier-Stokes (RANS) equations and gives information about the mean flow.

Although this approach is not able to describe the multitude of length scales involved in turbulence, it has been largely used all of the word because in many engineering applications the information about the mean flow is quite satisfactory.

Considering that density and viscosity variations are small so that their effects on turbulence can be ignored, the fluid is Newtonian and incompressible, and the steady state, the governing RANS equations in Cartesian coordinates can be expressed by (Versteeg and Malalasekera, 1995; CFX, 2003):

$$\frac{\partial U_i}{\partial x_i} = 0 \,, \tag{1}$$

$$\rho \frac{\partial (U_i U_j)}{\partial x_j} = -\frac{\partial P}{\partial x_i} + \frac{\partial}{\partial x_j}\left(\mu \frac{\partial U_i}{\partial x_j} - \rho \overline{u_i u_j} \right) + F_i \,, \tag{2}$$

where U_i and U_j are components of the average velocity vector [m/s], ρ is the fluid density [kg/m^3], μ is the dynamic viscosity of the fluid [Pa.s], P is the mean average pressure [Pa] and F_i is a component of the bulk force vector [N]. The extra-term that appears in Eq. (2) comparing to the original Navier-Stokes equations, $\overline{u_i u_j}$, is the product of fluctuation velocities [m^2/s^2] termed Reynolds stresses and is never negligible in any turbulent flow. It represents the increase in the diffusion of the mean flow due to the turbulence. Equations (1) and (2) can only be solved if the Reynolds stress tensor are known, a problem referred to as the 'closure problem' since the number of unknowns is greater than the number of equations.

The main goal of the turbulence studies based on the RANS equations is to determine the Reynolds stresses. According to Kolmogorov (1942) they can be evaluated by the following expression:

$$-\overline{u_i u_j} = \nu_t \left(\frac{\partial U_i}{\partial x_j} + \frac{\partial U_j}{\partial x_i} \right) - \frac{2}{3} \delta_{ij} k \,, \tag{3}$$

where δ_{ij} is the Kronecker delta and the kinetic energy of the turbulent motion, *k*, is defined as $k = \overline{u_i u_i}/2$ [m^2/s^2]. Substitution of Eq. (3) into Eq. (2) results in the average Navier-Stokes equations with the Reynolds stresses modeled via the viscosity concecpt,

$$\rho \frac{\partial (U_i U_j)}{\partial x_j} = -\frac{\partial P'}{\partial x_i} + \frac{\partial}{\partial x_j}\left[(\mu + \mu_t)\left(\frac{\partial U_i}{\partial x_j} + \frac{\partial U_j}{\partial x_i} \right) \right] + F_i \tag{4}$$

where μ_t is the turbulent viscosity, F_i is a component of the bulk force vector [N], and $P' = P + 2/3k$ is the modified pressure.

The turbulent viscosity can be expressed as the product of a velocity scale, *u* [m/s], and a length scale, L_μ [m], $\mu_t = \rho u L_\mu$. Considering the velocity scale being calculated by $u = k^{1/2}$, Kolmogorov (1942) and Prandtl (1945) independently proposed the following relation for the turbulent viscosity,

$$\mu_t = \rho c_\mu k^{1/2} L_\mu , \tag{5}$$

where c_μ (=0.09) is an empiric constant.

To close the set of equations described above, the most popular turbulence models define two other transport equations: one for the turbulent kinectic energy, *k*, and another for a variable that relates *k* to L_μ. These models are called two equations models, and three of them have been employed in this work: the standard *k*-ε model (Launder and Spalding, 1974), the RNG- *k*-ε model (Yakhot *et al*., 1992) and the *k*-ω model (Wilcox, 1988).

2.2 Two-equation turbulence models

Explicit formulations for three turbulence models: *k*-ε*, RNG k*-ε *and k*-ω are described below.

2.2.1 *k*-ε model

Due to its robustness, economy and acceptable results for a considerable amount of flows the *k*-ε model has been the most used model for numerical predictions of industrial flows. However, it is known to have deficiencies in some situations involving streamline curvature, acceleration and separation. This model will be used because is the turbulence model frequently used in the same computational domain adopted in this work

In this model, proposed by (Launder and Spalding, 1974), the second variable for the complementary transport equations is the rate of the viscous dissipation, ε [m^2/s^3], which is related to *k* by:

$$\varepsilon = k^{3/2}/L . \tag{6}$$

Therefore, the set of equations concerning the standard *k*-ε model is composed of Eqs. (1), (4) and (5), Eq. (6), and two transport equations for *k* and ε that are, respectively, given by:

$$\rho \frac{\partial (U_j k)}{\partial x_j} = \frac{\partial}{\partial x_j}\left[\left(\mu + \frac{\mu_t}{\sigma_k} \right) \frac{\partial k}{\partial x_j} \right] + \mu_t \left[\frac{\partial U_i}{\partial x_j} + \frac{\partial U_j}{\partial x_i} \right] \left[\frac{\partial U_i}{\partial x_j} \right] - \rho\varepsilon \tag{7}$$

$$\rho \frac{\partial (U_j \varepsilon)}{\partial x_j} = \frac{\partial}{\partial x_j}\left[\left(\mu + \frac{\mu_t}{\sigma_\varepsilon} \right) \frac{\partial \varepsilon}{\partial x_j} \right] + c_1 \mu_t \frac{\varepsilon}{k} \left[\frac{\partial U_i}{\partial x_j} + \frac{\partial U_j}{\partial x_i} \right] \left[\frac{\partial U_i}{\partial x_j} \right] - c_2 \rho \frac{\varepsilon^2}{k} \tag{8}$$

where c_1 = 1.42; c_2 = 1.92; σ_k = 1 e σ_ε = 1.22 are empirical constants.

As Eqs. (7) and (8) cannot describe correctly the movement of the fluid near solid surfaces, the so called wall-functions are required to make it applicable to the entire domain.

2.2.2 *RNG k*-ε model

Yakhot *et al.* (1992) have derived a new form of *k*-ε model from the governing equations for the fluid motion using Renormalization Group (RNG) methods. In this method constants and functions are evaluated by the theory and not by

empiricism, and the model can be applied to the near-wall region without recourse to wall-functions or ad-hoc function in the transport equations of the turbulence quantities. Some examples of flows where the *RNG k-ε* model has been seen to return better predictions than the standard *k-ε* are those including flow separation, streamline curvature and flow stagnation. In this model the same set of equations of standard *k-ε* model is used, Eqs. (1), (4) and (7)–(8).

Thus, basically the difference between the two models consists in the coefficients. For the RNG *k-ε* model the coefficients are obtained theoretically and are defined as c_μ = 0.0845, c_2 = 1.68, σ_k = 0.7194, σ_ε = 0.7194, and $c_1 = 1.42 - f_\eta$, where,

$$f_\eta = \frac{\eta\left(1-\frac{\eta}{4{,}38}\right)}{(1+\beta\eta^3)}, \tag{9}$$

$$\eta = \sqrt{\frac{\mu_t\left(\frac{\partial U_i}{\partial x_j}+\frac{\partial U_j}{\partial x_i}\right)\left(\frac{\partial U_i}{\partial x_j}\right)}{\rho C_\mu \varepsilon}}, \tag{10}$$

with β = 0.012.

2.2.3 *k-ω* model

Kolmogorov (1942) proposed the first two-equation model of turbulence, which included one differential equation for *k* and a second for ω, defined as the rate of dissipation of energy per unit volume and time. Saffman (1970) independently formulated a similar two-equation *k–ω* model. The parameter ω can be considered "a frequency characteristic of the turbulence decay process" (Saffman, 1970) and is related to dissipation by

$$\omega = \frac{\varepsilon}{c_\mu^4 k}. \tag{11}$$

Wilcox and Alber (1972), Saffman and Wilcox (1974), and others cited in Wilcox (1998) have provided further improvements to the model. The version of the *k–ω* model presented by Wilcox (1988), who formulated a low Reynolds number alternative to the standard *k- ε* turbulence model, is the one used here.

Wilcox (1988) proposed that the dissipation-rate equation of the *k-ε* model be replaced by an equation for a specific dissipation rate defined as $\omega = k/\varepsilon$. This *k-ω* model predicts the behaviour of attached boundary layers in adverse pressure gradients more accurately than *k-ε*. models, but performs poorly in free shear flows (Bardina *et al.*, 1997). The vorticity, ω, is associated to the turbulent kinectic energy, *k*, by the following expression:

$$\mu_t = \rho\frac{k}{\omega}. \tag{12}$$

Thus, in the model proposed by Wilcox (1988) the transport equations for the turbulent kinetic energy *k* and the specific dissipation rate ω are defined by Eqs. (13) and (14), respectively,

$$\rho\frac{\partial(U_j k)}{\partial x_j} = \frac{\partial}{\partial x_j}\left[\left(\mu+\frac{\mu_t}{\sigma_k}\right)\frac{\partial k}{\partial x_j}\right] + \mu_t\left[\frac{\partial U_i}{\partial x_j}+\frac{\partial U_j}{\partial x_i}\right]\left[\frac{\partial U_i}{\partial x_j}\right] - \beta_1\rho k\omega. \tag{13}$$

$$\rho\frac{\partial(U_j \omega)}{\partial x_j} = \frac{\partial}{\partial x_j}\left[\left(\mu+\frac{\mu_t}{\sigma_\omega}\right)\frac{\partial \omega}{\partial x_j}\right] + \alpha\mu_t\frac{\omega}{k}\left[\frac{\partial U_i}{\partial x_j}+\frac{\partial U_j}{\partial x_i}\right]\left[\frac{\partial U_i}{\partial x_j}\right] - \beta_2\rho\omega^2, \tag{14}$$

where σ_k = 2, σ_ω = 2, β_1 = 0.09, β_2 = 0.075 and α = 5/9.

The main problem with the Wilcox model is its well known strong sensitivity to free stream values of ω. Depending on the value specified for ω at the inlet, a significant variation in the results of the model can be obtained. A possible solution to this deficiency is to use a combination of the *k-ω* model equations implemented near wall regions and the *k-ε* turbulence model to be employed in the bulk flow region. This leads Menter (1992) to formulate the Shear-Stress Transport (SST) turbulence model that not is investigated here.

3. NUMERICAL METHODOLOGY

The numerical solution of the governing equations was performed using the commercial computational fluid dynamics code CFX, version 5.7.1 (2003). In this code the conservation equations for mass, momentum and turbulence quantities are solved using the finite volume discretization method *generated by unstructured Voronoi Diagram*. For this practice the solution domain is divided in small control volumes, using a non-staggered grid scheme, and the governing differential equations are integrated over each control volume with use the Gauss' theorem. The resulting discrete system of linearised equations is solved using an Algebraic Multigrid called Additive Correction accelerated Incomplete Lower Upper (ILU) factorisation technique. It is an iterative solver whereby the exact solution of the equations is approached during the course of several iterations.

In the method adopted in this work interpolation of properties at the control volume faces can be of primary importance on the accuracy of the numerical results. The classical approach of first order accurate upwind differencing usually suffers from inaccuracies in complex flow situations. An effective approach to reduce truncation error, while still maintaining the grid size within computational resource limits, is the adoption of a more accurate differencing scheme into the numerical analysis. In the present work, the first order Upwind Difference Scheme (UDS) is adopted firstly in the solution of the momentum equations, after such values are used as initial values for the High Resolution Scheme. The high resolution scheme is therefore both accurate (reducing to first order near discontinuities and in the free stream where the solution has little variation) and bounded. Therefore your order accuracy for the interpolated values can be major that two.

Three grid levels formed by 200.435, 382.887 and 918.145 volumes were used in domain with 100% of width of the inlet slot while 199.854, 381.246 and 915.165 volumes were used in domain with 50% of width of the inlet slot, to assess the numerical truncation error, for *k-ε* and RNG *k-ε* models. Each grid is denominated case 1, case 2 and case 3, in this sequence, respectively. The refinement was mainly promoted in the entrance and walls of the environment, where flow property gradients are steeper. The simulation stops when the normalized residual, Eq. (15), attains 10^{-5}.

$$\tilde{r}_\phi = \frac{r_\phi}{a_p \Delta\phi} < \gamma \tag{15}$$

where r_ϕ is the raw residual control volume imbalance, a_p is representative of the control volume coefficient, $\Delta\phi$ is a representative range of the variable in the domain, ϕ represents all variables and $\gamma = 10^{-5}$ is the stopping criterion.

4. RESULTS AND DISCUSSIONS

4.1 Problem description

The experimental data from Nielsen (1990) were used to check the numerical results. The measurements were carried out in a rectangular scaled-down room where the air enters horizontally at the top of one side and leaves the room at the bottom of the opposite side. Figure 1 shows a sketch of this experimental device, as well as the positions in which the mean velocity profiles were compared in two planes z/W = 0.4 and z/W = 0.5 (central plane).

In this work, the CFD simulations were conducted in the full-scale geometry equivalent to the Nielsen's experiment with the following dimensions: height H=3.0 m, length L = 3.0H, inlet height h = 0.056H and outlet height t = 0.16H. The Reynolds number is 5,000, based on the inlet height.

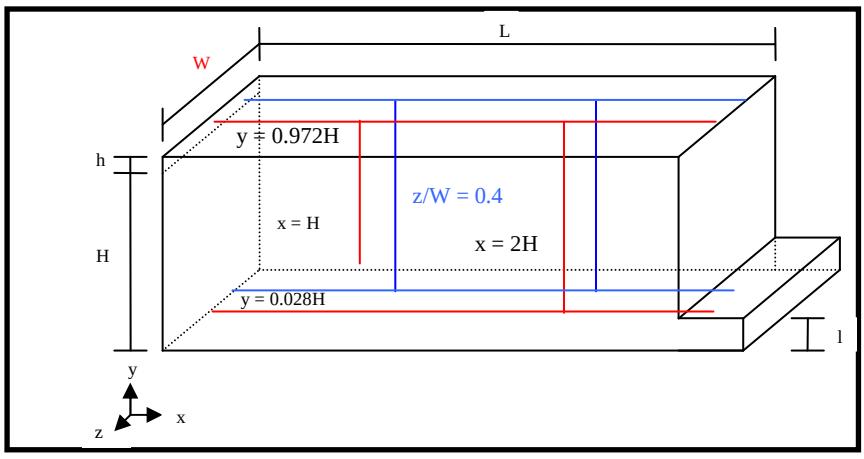

Figure 1. Flow geometry.

The inlet boundary conditions for the x direction, y direction and z direction velocity components were specified as $U = U_0$ and $V = W = 0$, respectively, with U_0 being the air average velocity in the inlet of the cavity, obtained by Reynolds number as $U_0 = \nu Re/h$. The inlet boundary conditions for the k and ε were measured by laser-Doppler anemometry and the data are in Restivo (1979), such values are assumed as $k_0 = 1.5(0.04U_0)^2$ and $\varepsilon_0 = 10k^{3/2}/h$. Therefore, the vorticity was used as $\omega_0 = k_0/L^2$. Zero relative pressure and zero gradients for the other variables are applied as the boundary conditions for the air outlet. At the solid boundaries the no-slip and the impermeable wall boundary conditions were imposed for the velocity components, that is, $U = V = W = 0$. The turbulence quanties k, ε and ω are nulls at the walls.

4.2 Result analysis

The flow through the room in Fig. 1 was investigated for one Reynolds number, Re = 5000 and two width of the inlet slot, 100% and 50%, and three turbulence models k-ε standard, RNG k-ε and k-ω. In all cases, the room dimensions were mantained with constant values.

The numerical solution was validated by means of sensitivity tests of the results with respect to grid refinement. The numerical validation and turbulence models assessment were conducted with reference to results of mean velocity profiles in four different positions, see details in Fig. 1.

For to choice the grid more adapted for domain with width of the inlet slot of 100% was realized. In this context, a comparison of velocity predictions by different grids with experimental data along the vertical and horizontal lines is presented in Fig. 2 for k-ε model. In Fig. 2 note that the case 3 (48900 volumes) gives satisfactory agreement with the experiment. These tests were made with the other two turbulence models supplying satisfactory results, except for the RNG k-ε model. These results suggest that intermediate-grid is a potential candidate for predictions of the airflows in room.

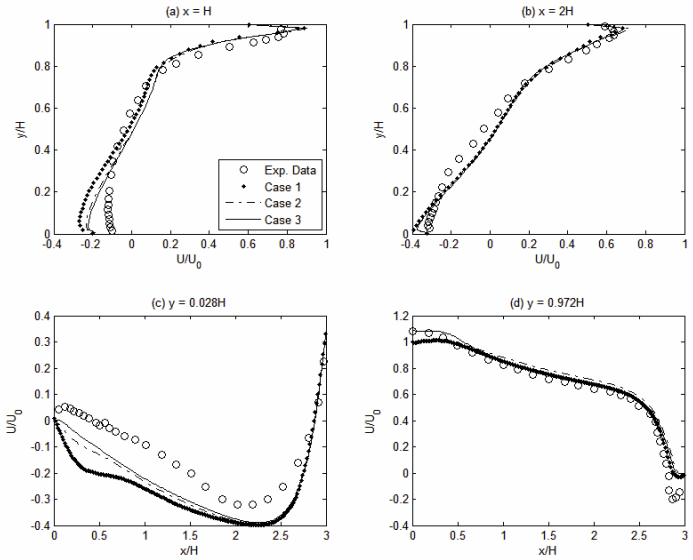

Figure 2. Comparison of velocity profiles predicted by k-ε model with the experimental data for z/W=0.5.

Figure 3 the numerical dimensionless mean velocity profiles obtained with the three turbulence models are compared to the experimental data at the four lines x = H, x = 2H, y = 0.028 H and y = 0.0972H in the central plane for width of the inlet slot equals 100%. The Fig. 4 shows a similarly comparison for the plane z/W = 0.4. One can observe from Figs. 3 and 4 that the standard k-ε and k-ω models agree better with the experimental results than the RNG k-ε model, we believe that this occurs because the used grid is not again adjusted mainly for the RNG k-ε model.

In the two planes, at the positions x = H and x = 2H, the standard k-ε model reproduced quite well the behaviour of the experimental data, except near the floor, at the position x = H in the plane z/W = 0.4, where it overpredicted the velocity. At these positions, the k-ω model shows slightly worse accordance with the measurements than the standard k-ε model. It overpredicted the velocity close to the floor in both planes at the position x = H.

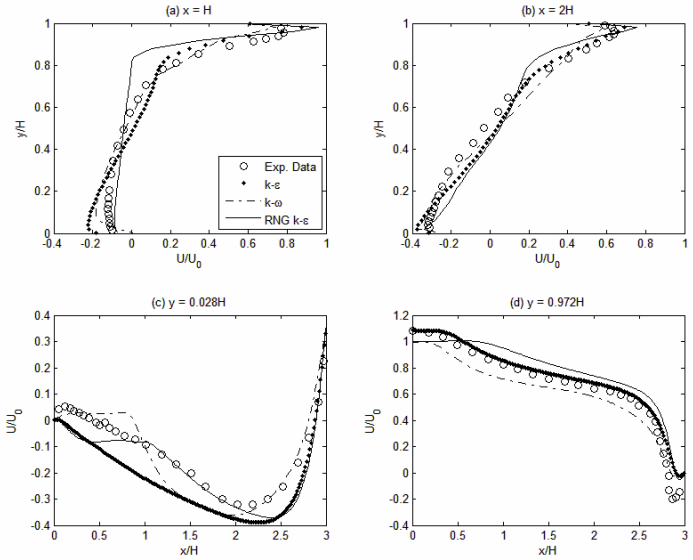

Figure 3. Comparison of velocity profiles predicted by turbulence models with the experimental data for z/W = 0.5.

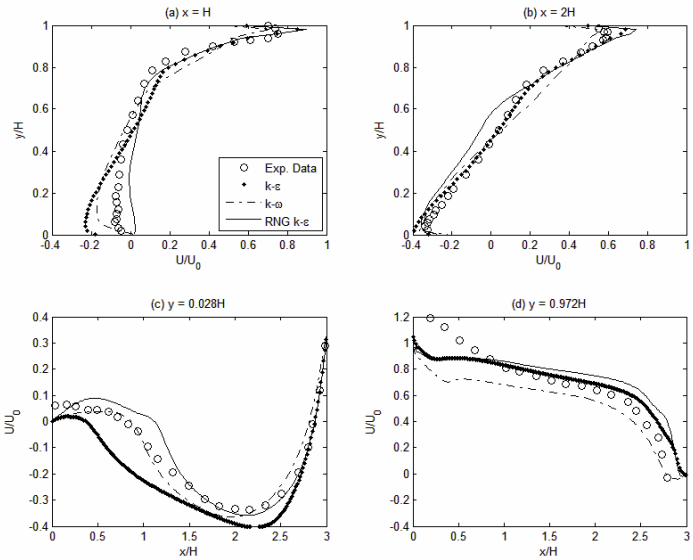

Figure 4. Comparison of velocity profiles predicted by turbulence models with the experimental data for z/W = 0.4.

Figs. 3c and 4c show that close to the floor, at the left bottom of the room, the k-ω model slightly overpredicted the velocity. On the other hand, close to the ceiling, this model underpredicted the velocity in the two corners of the room, In the region of high velocities, near the ceiling, the agreement between the numerical and the experimental results for the RNG k-ε model was as good as that for the standard k-ε model. Furthermore, the k-ω model was able to predict the recirculation in the upper right corner of the room, even though the velocity was underpredicted in this zone. The biggest discrepancies between numerical results and measurements for the k-ω model were found close to the floor in the central plane, Fig. 3c. In the other plane, z/W = 0.4, at y = 0.028 H, the behaviour of the experimental curve was slightly better reproduced by this model. In Fig. 3d and 4d the model k-ω underpredicts the velocity profiles while the RNG k-ε and k-ε models overpredict. As shown in Figs. 3 and 4 the predictions obtained with the RNG k-ε model agreed poorly with measurements, new finer grids should be analysed in a future work. Comparing the Figs. 3 and 4 that present profiles of the longitudinal velocity component at two values of z, the measurements confirm that the flows is symmetric about the mid plane within measurement precision, suggesting that, in region -0.4 < z/W < 0.4, the flow is closed to two-dimensional, as observed by Nielsen *et al.* (1978).

Thus, the next step in the analysis was to generate the numerical simulations for some flow situations not included in the experimental investigation. The computations were then conducted for width of the inlet slot of 50%. Newly for to choice the grid more adequate for domain with width of the inlet slot of 50% a comparison of velocity predictions by different grids with experimental data along the vertical and horizontal lines is presented in Fig. 5 for k-ε model. In this

figure note that the case 3 gives satisfactory agreement with the experiment. In similar way, the 100% slot the RNG k-ε model has not satisfactory results. Thus the finer-grid was used for predictions of the airflows in room. In Fig. 6a and 6b the modelo k-ε predicts the velocity correctly and perform better than the RNG k-ε and k-ω models, except in the region near top wall, where the value is underpredicted.

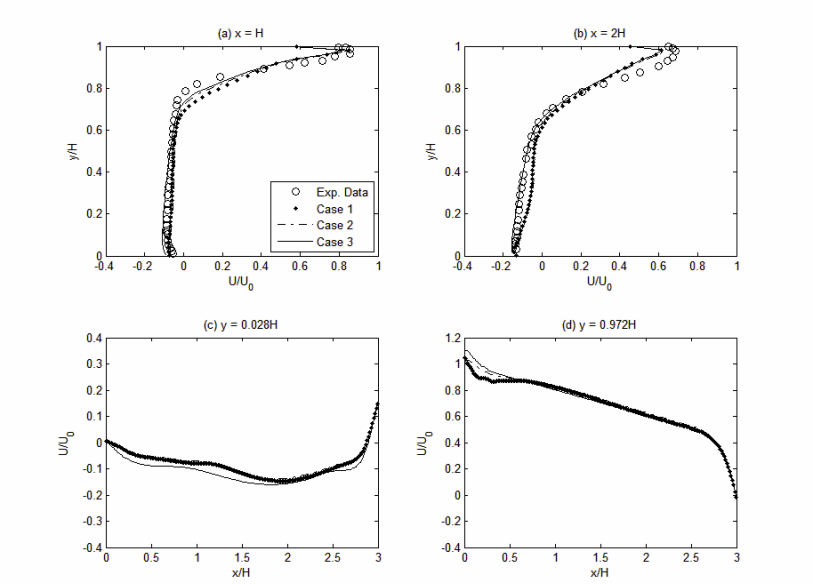

Figure 5. Comparison of velocity profiles predicted by k-ε model with the experimental data for z/W = 0.5.

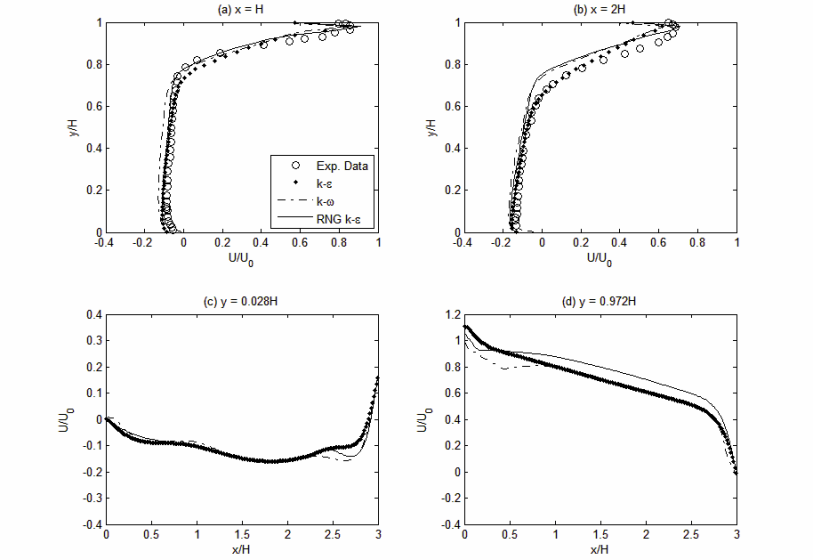

Figure 6. Comparison of velocity profiles predicted by turbulence models with the experimental data for z/W = 0.5.

In the region of high velocities, near the ceiling, the agreement between the numerical and the experimental results for the k-ω model was as that for the standard k-ε model, as presented in Fig. 6. The Fig. 7 presents results for z/W = 0.4 where for the shorter slot in the room, the velocity profiles show clearly that the flow is three-dimensional when compared with the Fig. 5. The biggest discrepancies between numerical results and measurements were for the RNG k-ε model close to the floor in x = H and close to the ceiling in x = 2H in the central plane, see Figs. 7a and 7b, respectively. In same plane, at y = 0.028 H and y = 0.972H the models k-ε and k-ω have similar behaviour while the RNG k-ε model no agree with the others models. As shown in Figs. 3 and 4 the predictions obtained with the RNG k-ε model agreed poorly with experimental data. Comparing Figs. 4 and 6, for two inlet arrangements, note that the velocity profiles are differents in the central plane main close to the floor. For Figs. 5b, 5c, 6b and 6c no reported results were found in the literature which could be used for comparison purposes.

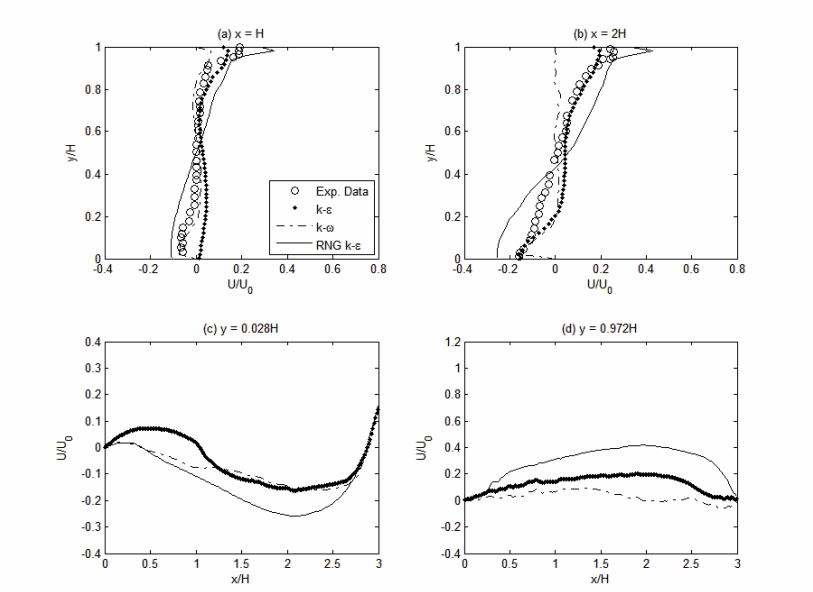

Figure 7. Comparison of velocity profiles predicted by turbulence models with the experimental data for z/W = 0.4.

In this work is desired to minimize the difference between experimental and predicted velocities, such deviations was calculated by mean square error, $MSE = \frac{1}{N}\sum_{j=1}^{N}\left[u_{exp}^{j} - u_{num}^{j}\right]^2$, where $u_{exp} = (U/U_0)_{exp}$ is the experimental velocity in position j, $u_{num} = (U/U_0)_{num}$ is velocity calculated numerically by turbulence models in the same position and N is the sample number. The Fig. 8 shows results for *MSE* conducted for width of the inlet slot of 100% and 50%, respectively, for position x = H and all turbulence models, where can be see which the grid represented by case 3 is the more appropriate.

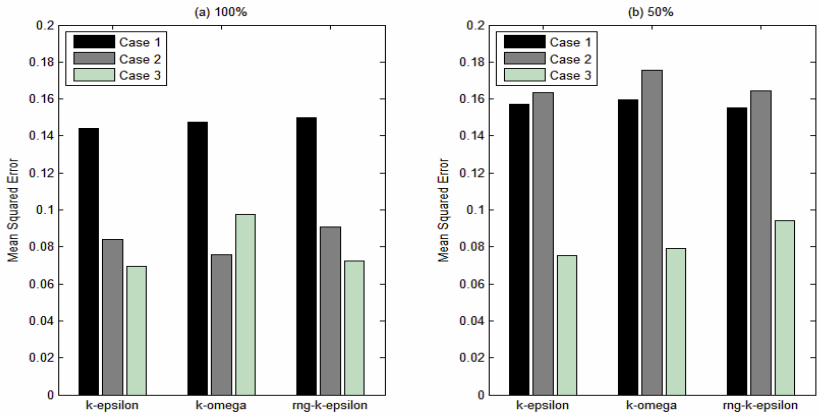

Figure 8 – Mean square error for z/W = 0.5.

5. CONCLUSIONS

The work has presented a numerical investigation of the incompressible turbulent and isothermal air flow in a room. The prediction of the mean velocity by the three turbulence models is generally satisfactory for k-ε and k-ω models, agree with the experimental data, and unsatisfactory for RNG k-ε model. Since that all models use the assumption of isotropic turbulence, they also fail to predict correctly the anisotropic turbulence found in indor air flow. New simulations should be made with the model RNG k-ε because this model is recommended in other works for simulations of indoor air flow, believe that finer grid can better its performance.

6. ACKNOWLEDGEMENTS

The authors would like to acknowledge *Coordenação de Aperfeiçoamento de Pessoal de Nível Superior*, CAPES, for the scholarship provided to the first author of this paper, and *Fundação Araucária* for its financial support for this work.

7. REFERENCES

Bardina, J. E., Huang, P. G. and Coakley, T. J., 1997, "Turbulence modeling validation, testing, and development", *NASA-TM-110446*.

Chen, Q., 1995, "Comparison of different k-ε models for indoor air flow computations", Numerical Heat Transfer, Part B, Vol. 28, pp. 353-369.

Chen, Q., 1996, "Prediction of room air motion by Reynolds-stress models", Building and Environment, Vol. 31, pp. 233-244.

Chen, Q. and Xu, W., 1998, "A zero-equation turbulence model for indoor airflow simulation", Energy and Buildings, Vol. 28, pp. 137-144.

Dirichlet, G. L., 1850, Uber die Reduction der positiven quadratschen formen mit drei undestimmten ganzen Zahlen, Z. Reine Angew, Math., Vol. 40, pp. 209-227.

Kolmogorov, A.N., 1942, "Equations of turbulent motion of an incompressible fluid". Izvestia Acad. Sci., USSR; Phys. Vol. 6, pp. 56–58.

Launder, B. E., 1989, "Second-moment closure: present…and future?" International Journal of Heat Fluid Flow, Vol.10, pp. 282-300.

Launder, B. E. and Sharma, B. I., 1974, "Application of the energy dissipation model of turbulence to the calculation of flow near spinning disc". Letters in Heat and Mass Transfer, Vol. 1, pp. 131-138.

Launder, B. E. and Spalding, D. B., 1974, "The numerical computation of turbulent flows", Comp. Meth. Appl. Mech. Energy, Vol. 3, pp. 269-289.

Menter, F. R., 1992, "Improved two-equation k-ω turbulence model for aerodynamic flows", NASA TM-103975, 1992.

Menter, F. R., 1993, "Zonal two k-ω turbulence model for aerodynamic flows", AIAA, 24th Fluid Dynamics Conference, Florida, pp.1-21.

Menter, F. R., 1994, "Two-equation eddy viscosity turbulence models for engineering applications", AIAA Journal, Vol. 32, pp. 1598-1605.

Moureh, J. and Flick D., 2003, " Wall air-jet characteristics and airflow patterns within a slot ventilated enclosure", International Journal of Thermal Sciences, Vol. 42, pp. 703-711.

Nielsen, P. V., 1990, "Specification of a two-dimensional test case", Technical report, International Energy Agency, Annex 20: Air Flow Pattern Within Buildings.

Nielsen, P. V., Restivo, A. and Whitelaw, J. H., 1978, "The velocity characteristics of ventilated rooms", Journal of Fluid Engineering, Vol. 100, pp. 291-298.

Patankar, S. V., 1980, "Numerical Heat Transfer and Fluid Flow", McGraw-Hill.

Prandtl, L., Wighardt, K., 1945, "Über ein neues formelsystem für die ausgebildete turbulenz", Nachr. Akad. Wiss., Math.-Phys, Kl., 6.

Restivo, A., 1979, "Turbulent flow in ventilated rooms", Ph. D. thesis, University of London, U.K.

Reynolds, O., 1895, "On the dynamical theory of incompressible viscous fluids and the determination of the criterion", Phil. Trans. Roy. Soc. London Ser.A, Vol. 186, pp. 123-164.

Saffman, P.G., 1970, "A model for inhomogeneous turbulent flow". Proc. R. Soc., Lond. A 317, pp. 417–433.

Saffman, P.G. and Wilcox, D.C., 1974, "Turbulence-model predictions for turbulent boundary layers". AIAA Journal, Vol. 12, pp. 541–546.

Schälin, A. and Nielsen, P. V., 2004, "Impact of turbulence anisotropy near walls in room airflow", Indoor Air, Vol. 14, pp. 159-168.

Versteeg, H. K. and Malalasekera, W., 1995, "An introduction to computational fluid dynamics", Longman Scientific & Technical, New York.

Voigt, L. K., 2000, "Comparasion of turbulence models for numerical calculation of airflow in an annex 20 room", Technical report, Technical University of Denmark.

Wilcox, D.C. and Alber, I.E., 1972, "A turbulence model for high speed flows". In: Proc. of the 1972 Heat Trans. & Fluid Mech. Inst.. Stanford Univ. Press, Stanford, CA, pp. 231–252.

Wilcox, D.C., 1988, "Reassessment of the scale determining equation for advance turbulence models". AIAA Journal, Vol. 26, pp. 1299–1310.

Wilcox, D.C., 1998. "Turbulence modeling for CFD". DCW Industries, Inc, La Canada, CA. p. 540

Xu, W. and Chen, Q., 2001a, "A two-layer turbulence model for simulation indoor airflow Part I. Model development", Energy and Buildings, Vol. 33, pp. 613-625.

Xu, W. and Chen, Q., 2001b, "A two-layer turbulence model for simulation indoor airflow Part II. Applications", Energy and Buildings, Vol. 33, pp. 627-639.

Yakhot, V., Orszag, S. A., Thangam, S., Gatski, T. B. and Speziale, C. G., 1992, "Development of turbulence models for shear flows by a double expansion technique", Phys. Fluids A, Vol. 4, pp. 1510-1520.

8. RESPONSIBILITY NOTICE

The authors are the only responsible for the printed material included in this paper.